Available online at www.sciencedirect.com

ScienceDirect

Energy Procedia 54 (2014) 400 – 416

Energy Procedia

4th International Conference on Advances in Energy Research 2013, ICAER 2013

# Numerical Investigation of Micro-channel Based Active Module Cooling for Solar CPV System

K. S. Reddy[a*], S. Lokeswaran[a], PulkitAgarwal[a], Tapas K. Mallick[b]

[a]*Heat Transfer and Thermal Power Laboratory, Department of Mechanical Engineering*
*Indian Institute of Technology Madras, Chennai - 600 036, India*
[b]*Environment and Sustainability Institute, University of Exeter, Cornwall, UK*

**Abstract**

Concentrating photovoltaic (CPV) technology is one of the fastest growing solar energy technologies achieving higher electrical conversion efficiencies. The increase in temperature of solar CPV cell significantly reduces the performance; the efficiency of a CPV system can be improved by introducing effective thermal management or cooling system. This paper presents the design and numerical analysis of a heat sink based on micro-channels for efficient cooling of a commercial high concentration photovoltaic (HCPV) cell. A combinatory model of an array of micro-channels enclosed in a wide parallel flow channel design is developed. The optimized geometry of the micro-channel heat sink was found by using commercial CFD software ANSYS 13. Based on numerical simulations, it is found that the optimum configuration of micro-channel with 0.5mm width and aspect ratio of 8. The micro-channels provided high heat transfer over heat generations spots and parallel flow channels resulted in lower pressure drop. The temperature rise across the micro-channel is estimated as10K in CPV module of 120 x 120 $mm^2$ and with a pressure drop of 8.5 kPa along a single channel with six such channels in each modules at a flow rate of 0.105 liter/s.



Selection and peer-review under responsibility of Organizing Committee of ICAER 2013

*Keywords:* Solar Energy; Concentrating Photovoltaic system; Microchannel Heatsink; NumericalAnalysis.

## 1. Introduction

Photovoltaic system converts solar energy into electrical energy bypassing the typical chain of conversions and energy losses that are associated with conventional power generation. Due to the high cost and lower conversion efficiency of PV cells, it referred as one of the most expensive renewable energy technologies. The cost of solar PV based electricity generation can be reduced by replacing semiconductor material with cheaper concentrating mirrors

* Corresponding author. Tel: 044-22574702;
E-mail: ksreddy@iitm.ac.in


Selection and peer-review under responsibility of Organizing Committee of ICAER 2013
doi:10.1016/j.egypro.2014.07.283

or lenses. Since the solar cell output depends on the magnitude of incident radiation, the CPV cell converts the incident solar energy to fraction of electrical energy and the remaining as thermal energy. This allows a 500–1000× reduction in semiconductor material by replacing it with low-cost recyclable alternatives for similar output ratings and is referred as Concentrating Photovoltaic (CPV) system. It addresses the important concerns for PV technology: the cost and efficiency. In order to utilizes the solar spectrum more effectively than traditional conventional PV, the CPV system uses multi-junction cells which consists of stack of *p–n* junctions composed of group III and V materials connected in series that are designed with different band gaps to absorb different parts of the solar radiation increasing the conversion efficiency. The highest photovoltaic cell efficiency recorded by using concentrating sunlight for multi junction cells is 43.5% (AMI 1.5d, 418 suns) [1]. Since the CPV cell operates at much greater irradiance levels compared to conventional PV, the cell temperature increases, which should be kept within limits for efficient and continuous operation of system. The photovoltaic cell efficiency decreases with increase in temperature; the non-uniform temperature across the cell limits the efficiency of the whole string due to the current mismatch. The cells will also exhibit long-term degradation if the temperature exceeds a certain limit. Thus, the cooling system of a CPV module is a very crucial design parameter. Royneet.al. [2] discussed the different cooling methods used for CPV applications. Depending on the cell arrangements they classified it as single-cell, linear, and densely packed cells. For the densely packed CPV module with concentration ratio over 500 suns, active cooling method with thermal resistance of less than $10^{-4}$ $m^2K/W$ is the only viable solution as the geometry of the cells limits the heat removal surface area.

The Various active cooling options used for densely packed CPV systems have been studied. Verlinden et al. [3] describes a 600 x 600 $mm^2$ wafer scale integrated silicon concentrator module of back contacted solar cells with a fully integrated water-cooled cold plate, which acts as a tile in a larger array. Lasich [4] has patented cooling circuit where water flowing through small, parallel channels extracts up to 500$kW/m^2$ from densely packed solar cells under high concentration maintaining the cell temperature around 40°C for normal operating conditions. Vincenzi et al. [5] have used micro-machined silicon heat sinks in their photovoltaic receiver of 300 x 300 $mm^2$ operating at a concentration 120 suns and reported thermal resistance of $4x10^{-5}Km^2/W$, that is comparable to other micro-channel systems. Min et al. [6] found that in micro channel heat sink, the added heat transfer through the fin tips lead to an increased heat sink performance and recommends to keep the channel width below 0.6. Alternating flow directions is one way of reducing the stream wise temperature gradient in the micro-channel heat sink. Numerical results by Vafai et al. [7] show that the stream wise temperature gradient is significantly lowered when two layers of counter-flow micro-channels are compared to a one-layer structure. This two layered design called the manifold micro-channel heat sink has been modeled and optimized by Ryu et al. [8], with laminar flow, it is shown that the thermal resistance is lowered by more than 50% compared to the traditional micro-channel heat sink, while drastically reducing the temperature variations on the base.

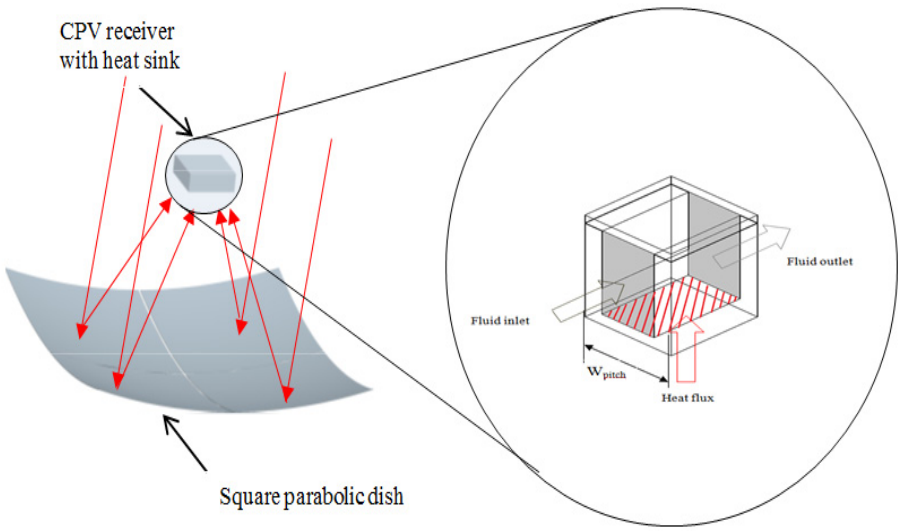

Fig.1.Solar CPV dish with micro-channel heat sink

A solar CPV receiver made of multi-junction photovoltaic cells has been designed and developed, which will deliver electricity and heat. The CPV module which consists of the CPV cell with substrate, secondary optics and cooling plate will be mounted on the focus of parabolic reflector as shown in Fig. 1. The reflective optics of the CPV dish of an area of $9m^2$ will focus the irradiation falling on the aperture to concentration ratio 500X at the receiver. Assuming an average solar irradiation of 550 $W/m^2$ the CPV module is capable of producing 1.5 $kW_e$ power and generates a maximum of 4.6 $kW_{th}$ of heat energy. Totally 144 solar cells are used in a 12 x 12 array mounted on dbc (direct bond copper) and the back side of the base is etched with micro-channels and covered with a plate to remove the heat produced and the whole system is encapsulated. The surplus heat will transfer from the cells to the cooling plate is by conduction through the substrate. The overall thermal resistance of the substrate is found from the thermal resistances of the individual layers (solder, substrate, and adhesive). The heat should be removed effectively, uniformly and continuously from the CPV cells for efficient working of CPV system.

In this paper, numerical analysis of micro-channel heat sink cooling system for high concentration solar CPV module has been carried out. Design and thermal management aspects of CPV cooling system have been investigated.

**Nomenclature**

| | |
|---|---|
| AS | Aspect ratio |
| $C_p$ | Specific heat (J/kg K) |
| $D_h$ | Hydraulic diameter (m) |
| E | Internal energy (J/kg) |
| F | Force (N) |
| H | Height of channel (mm) |
| K | Thermal conductivity (W/m K) |
| L | Length (mm) |
| $\dot{m}$ | Mass flow rate (kg/s) |
| P | Pressure (Pa) |
| Q | Heat flux ($W/m^2$) |
| Re | Reynolds number |
| T | Temperature (K) |
| T | Time (s) |
| $U_T$ | Temperature uniformity index (K) |
| U | x-direction velocity of liquid (m/s) |
| V | Velocity (m/s) |
| V | y-direction velocity of liquid (m/s) |
| W | width of channel (mm) |
| W | z-direction velocity of liquid (m/s) |

*Roman*

| | |
|---|---|
| ρ | Density ($kg/m^3$) |
| δ | Thickness of wall(mm) |
| μ | Viscosity (kg/m/s) |
| $\nu$ | Volume flow rate ($m^3/s$) |

*Subscripts*

| | |
|---|---|
| avg | average |
| In | inlet |

| | |
|---|---|
| L | liquid |
| max | maximum |
| min | minimum |
| N | normal |
| out | Outlet |
| S | Solid |
| W | Wall |
| W | work transfer |

## 2. Design and development of combinatory model for CPV cooling

A new combinatory model was developed by combining the merits of both the high heat removal effectiveness of micro/mini-channels with low pressure drops in conventional straight channels as reviewed in the literature. The combined model has micro-channel array directly below the surface where the CPV cells are mounted (heat spots) to remove the heat, where us in other regions since there is no heat generation conventional straight channels were used.

### *2.1. Design of Micro-channel Geometry*

The parallel micro-channel heat sink has been investigated to determine the optimal design under uniform power density applied from the bottom of the heat sink. The numerical model consists of a cell with single micro-channel array having series of parallel rectangular channel used in the current investigation is shown in Fig. 2. The base of the micro channel receives heat flux from the bottom surface and the heat is transferred directly to the coolant by convection from the base and indirectly through the dividing wall. The large surface area of micro channel enables the coolant to take away large amounts of heat per unit time per unit area while maintaining a considerably low device temperature. So, high heat fluxes can be dissipated at relatively low surface temperatures.

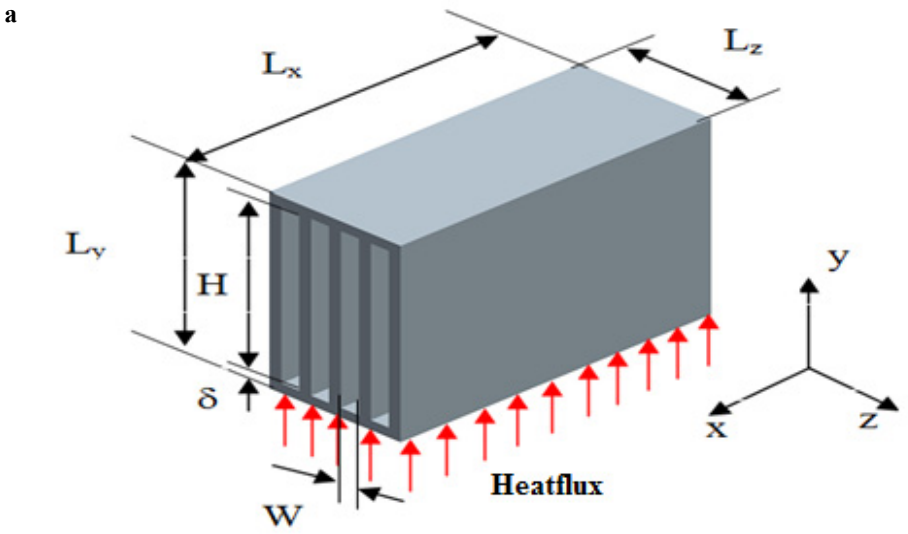


Fig. 2. Structure of a parallel micro channel heat sink.

### *2.2. Numerical simulation of micro-channel geometry*

The numerical simulation has been carried out with ANSYS 13 under steady, incompressible, laminar flow in the micro-channels for different Widths (0.2, 0.3, 0.4 mm), aspect ratio (0.2, 0.33, and 0.5) and Reynolds number (500, 1000, and 1500). The flow and heat transfer simulations are based on the simultaneous solution of governing conservation of mass, momentum and energy equations represented [8] as

Continuity equation

$$\frac{\partial m}{\partial t} = \sum_{in} \dot{m} - \sum_{out} \dot{m} \quad (1)$$

Momentum equation

$$\frac{\partial}{\partial t}(mV_n) = \sum F_n + \sum_{in} \dot{m}V_n - \sum_{out} \dot{m}V_n \quad (2)$$

Energy equation

$$\frac{\partial}{\partial t}(me) = \sum_{in} \dot{m}e - \sum_{out} \dot{m}e + \sum_i q_i - \sum_j w_j \quad (3)$$

The analysis was carried out using CFD software ANSYS 13 with SIMPLE algorithm for velocity-pressure coupling. The numerical solution was considered to be converged when the residual became smaller than 1 x $10^{-5}$ for the continuity and momentum equations and 1 x $10^{-9}$ for the energy equation. The Parameters used for micro channel heat sink simulations are listed in Table 1. The associated hydrodynamic and thermal boundary conditions are given in Table 2.

Table 1. Parameters used for micro-channel heat sink simulations.

| Properties of plate (Copper) | | Properties of coolant (water) at 40°C | |
|---|---|---|---|
| Parameters | Values | Parameter | values |
| Density ( $\rho$ ) | 8978 kg/m$^3$ | Density ( $\rho$ ) | 998.2 kg/m$^3$ |
| Specific heat ($C_{p,S}$) | 381 J/kg K | Specific heat ($C_{p,l}$) | 4182 J/kg K |
| Thermal conductivity ($K_p$) | 387.6 W/m K | Thermal conductivity ($K_w$) | 0.6 W/m K |
| | | Viscosity ($\mu_S$) | 0.000653 kg/m/s |

Table 2. Boundary conditions used in micro channel heat sink simulations.

| Hydrodynamic boundary conditions | | Thermal boundary conditions | | | |
|---|---|---|---|---|---|
| Channel wall surface | $u = v = w = 0$ | x=0, | if(y,z) channel $T_l=T_{in}$, else $-K_s \frac{\partial T_W}{\partial x} = 0$ | z=0, | $-K_S \frac{\partial T_W}{\partial z} = 0$ |
| Inlet | x = 0, $P=P_{in}$ | x=$L_x$, | if(y,z) channel $-K_l \frac{\partial T_l}{\partial x} = 0$, else $-K_S \frac{\partial T_W}{\partial x} = 0$ | z=$W_{pitch}$, | $-K_S \frac{\partial T_W}{\partial z} = 0$ |
| Outlet | x = $L_x$, $P=P_{out}$. | y=0, | $-K_S \frac{\partial T_W}{\partial y} = q_W$ | Inner surface | $-K_S \frac{\partial T_W(x)}{\partial n} = -K_l \frac{\partial T_l(x)}{\partial n}$ |
| | | y=$L_y$, | $-K_S \frac{\partial T_W}{\partial y} = 0$ | | |

The optimal design is determined by minimizing and comparing the following four parameters:

Pressure drop the micro channel ΔP,

Average temperature of the heat sink bottom defined as,

$$T_{avg} = \frac{\int_V T dv}{\int_v dv} \quad (4)$$

Temperature uniformity index $U_T$, defined as,

$$\frac{\int_V |T - T_{avg}| dv}{\int_v dv} \quad (5)$$

Surface temperature difference, $\Delta T = T_{max} - T_{min}$ (6)

### *2.3. Estimation of temperature rise and pressure drop across micro-channel*

The flow characteristics have been investigated in the micro-channels. The change in pressure drop (ΔP) with respect to Reynolds number is shown in Fig. 3. (a) . The pressure drop (ΔP) increases sharply with increase in Reynolds number. It decreases with increase in width and decrease in aspect ratio. ΔP decreases by seven times when width is doubled. To maintain low pressure drop the Reynolds number should be limited below 1500.The effect of aspect ratio of micro-channel on the temperature difference (ΔT), average temperature ($T_{avg}$) and temperature uniformity index ($U_T$) of the bottom surface is given in Fig. 3. (b) .Since ΔT , $T_{avg}$ and Temperature uniformity index $U_T$ of bottom surface decreases with decrease in the aspect ratio, for minimum ΔT (less than 1K) and lower $T_{avg}$ for bottom surface aspect ratio should be reduced which results in better performance. The variation of temperature difference (ΔT), average temperature ($T_{avg}$) and temperature uniformity index ($U_T$) of the bottom surface with respect to width and Reynolds number are shown in Fig.4. (a) and (b) . The temperature difference (ΔT) and temperature uniformity index ($U_T$) decreases with increase in width of micro-channel except $T_{avg}$, which increases linearly. Hence width should be increased within these limits. The ΔT, $T_{avg}$ and Temperature uniformity index $U_T$ decreases sharply with increase in the Re. But higher Re leads to higher ΔP across the micro-channel and laminar to transition flow which has to be avoided in order to keep pressure losses minimum. Hence, Re should be investigated within limits.

a

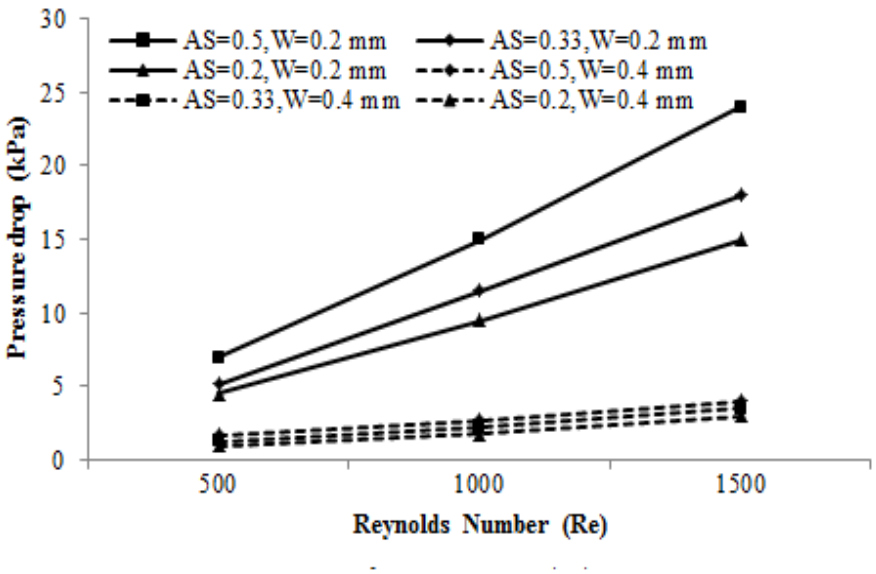

b

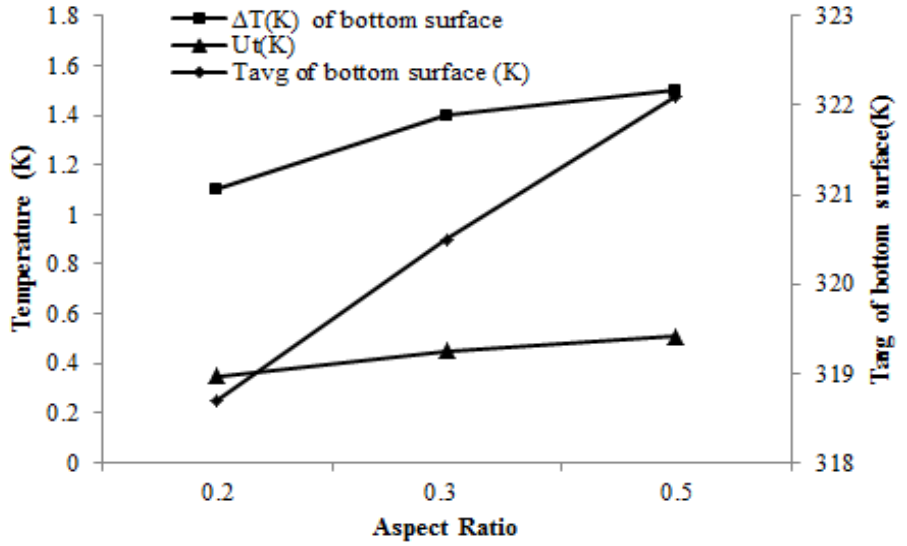


Fig. 3. (a) Effect of Reynolds number on pressure drop; (b) Effect of aspect ratio on ΔT , $T_{avg}$ and $U_T$.

a

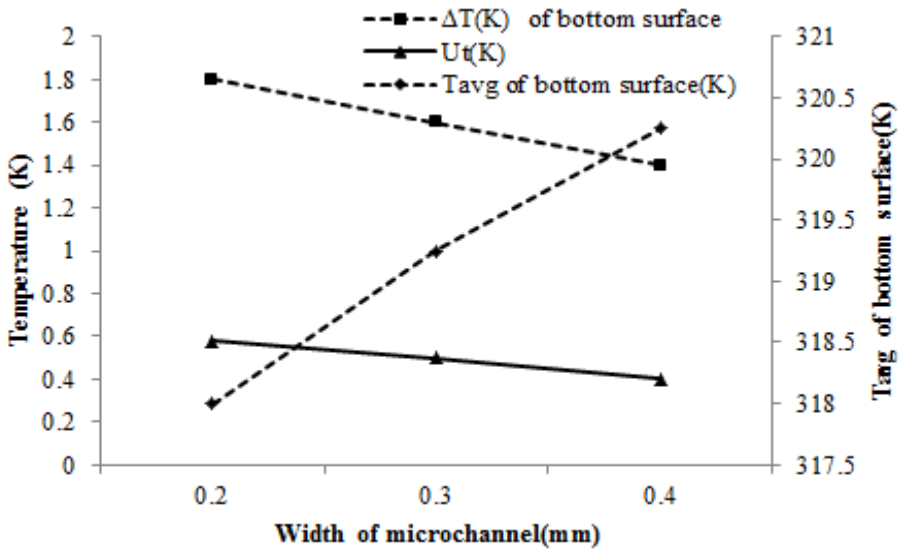

b

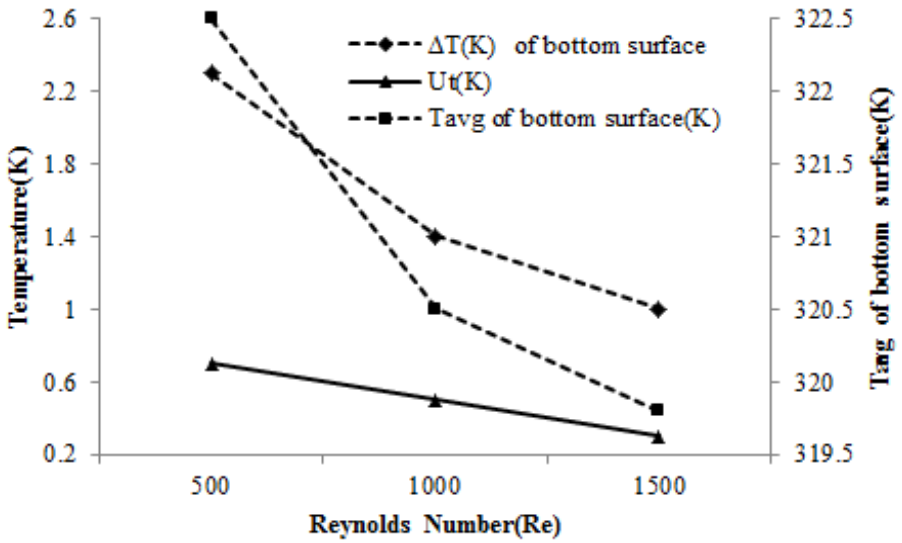


Fig.4. (a) Effect of width of micro channel on ΔT, $T_{avg}$ and $U_T$(K); (b) Effect of Reynolds number on ΔT ,$T_{avg}$ and $U_T$.

*2.4. Micro-channel geometry and pitch*

To find the effect of channel pitch on heat transfer the overall width of the micro channel array is taken as 12 mm because the PV cell width is also 12 mm (with tolerance). The simulation was carried out for width of 0.5 mm, pitch of 0.5mm, 0.30mm and 0.25 mm resulting in a micro-channel array of 12, 15 and 16 paths respectively and width of 0.4 mm pitch of 0.4mm, 0.35mm and 0.2 mm resulting in a micro-channel array of 15, 16 and 20 paths respectively The variation of temperature difference (ΔT), $U_T$ (K) of bottom surface and total Pressure Drop with respect to channel pitch are shown in Fig. 5. (a) , Fig. 5. (b) and Fig. 6 respectively. It is evident that the pitch variation does not have much impact on the ΔT, $U_T$ of the bottom surface but decrease in pitch results in higher volume flow rate leading to higher pressure drops across the micro channel array. Hence, micro channel of width 0.5 mm, pitch = 0.5 mm and aspect ratio, AS= 0.125 is selected for final analysis as this design has lowest pressure drop with comparable ΔT, $U_T$ and $T_{avg}$ of bottom surface.

a

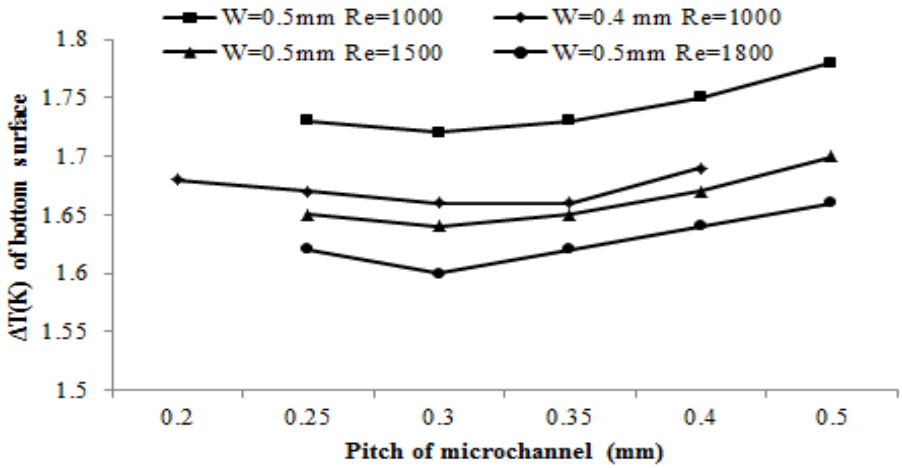

b

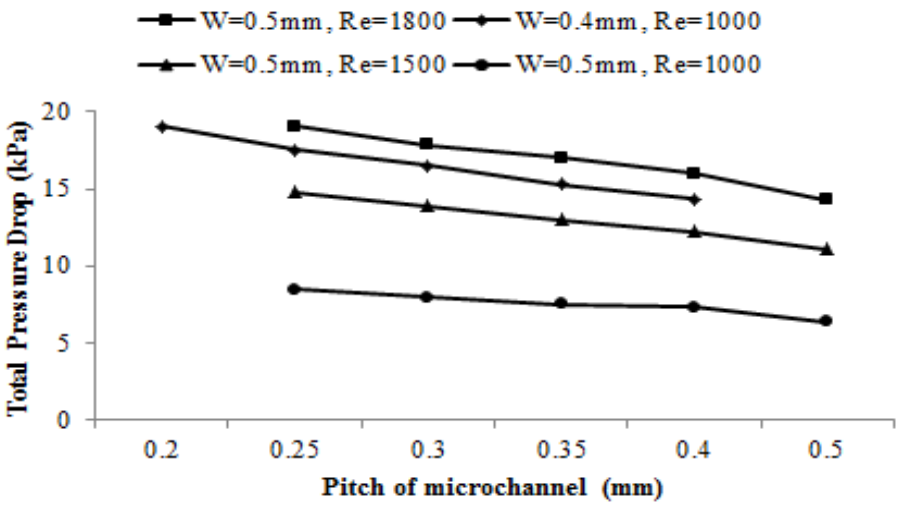


Fig. 5. Variation of (a) ΔT of bottom surface; (b) Total Pressure Drop with pitch of micro-channel.

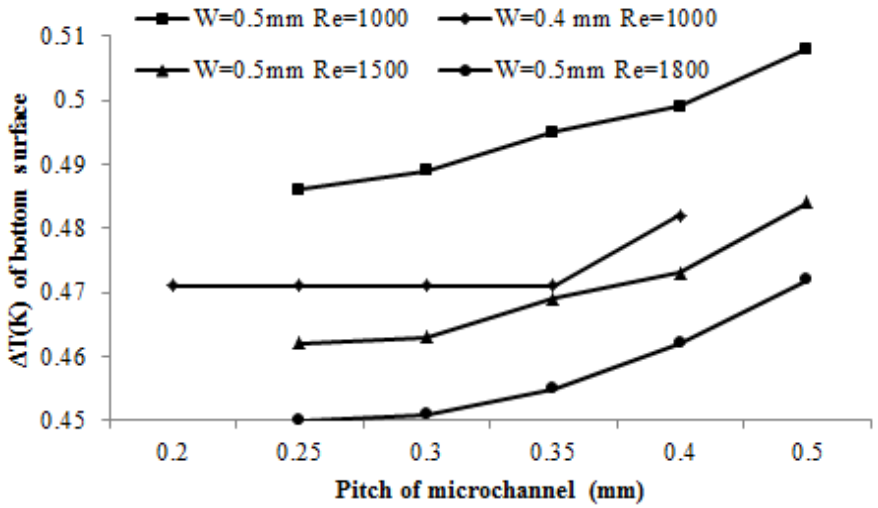


Fig. 6 Variation of $U_T$ (K) with pitch of micro-channel.

### *2.5. Analysis of profile region of micro-channel*

The wide straight flow channel comprises of two parts: the micro-channel array and the solid regions between the two subsequent micro-channels referred as the profile region. The dimensions of the profile region are fixed with 6mm width, 4mm depth and 8 mm length for interior profile regions (profile between any two micro-channel arrays) and 4 mm (inlet and outlet profile). The 2-D simulation was conducted for micro-channel and profile region together with quad-sub map mesh scheme for both laminar and transition flow. The SIMPLE algorithm was adopted to treat the pressure- velocity coupling with first order upwind scheme.

The pressure contours for micro channel and profile combined region under transition and laminar flow condition are shown in Fig. 7. The overall pressure drop in transition flow and laminar flow are comparable. The velocity contours for micro channel and profile combined region under transition and laminar flow condition are shown in Fig. 8. The pattern of isothermal lines on the flow path of all the channels are almost uniform and the velocity of the fluid increases from left to right profile region. The overall bulk velocity of both regions and profile exit velocity values are comparable as shown in Fig. 9, which indicates laminar flow to be more consistent with the previous 3-D micro-channel velocity profile results. Hence, the final micro channel of width = 0.5mm, depth = 4mm, pitch of 0.5 mm and length of 12 mm was used for cooling module.

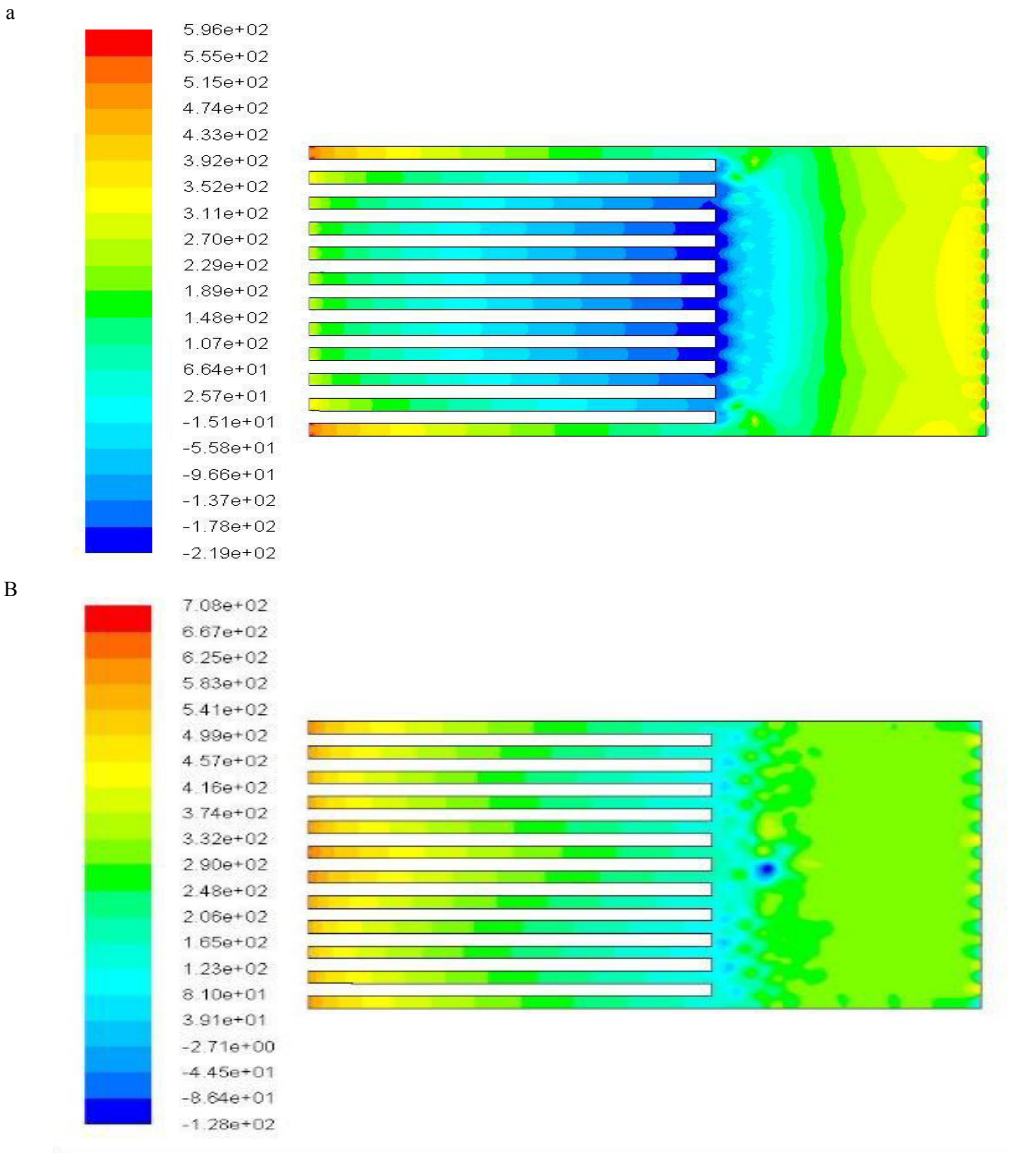


Fig. 7. Pressure contours of micro-channel and profile region in (a) transition and (b) laminar flow conditions

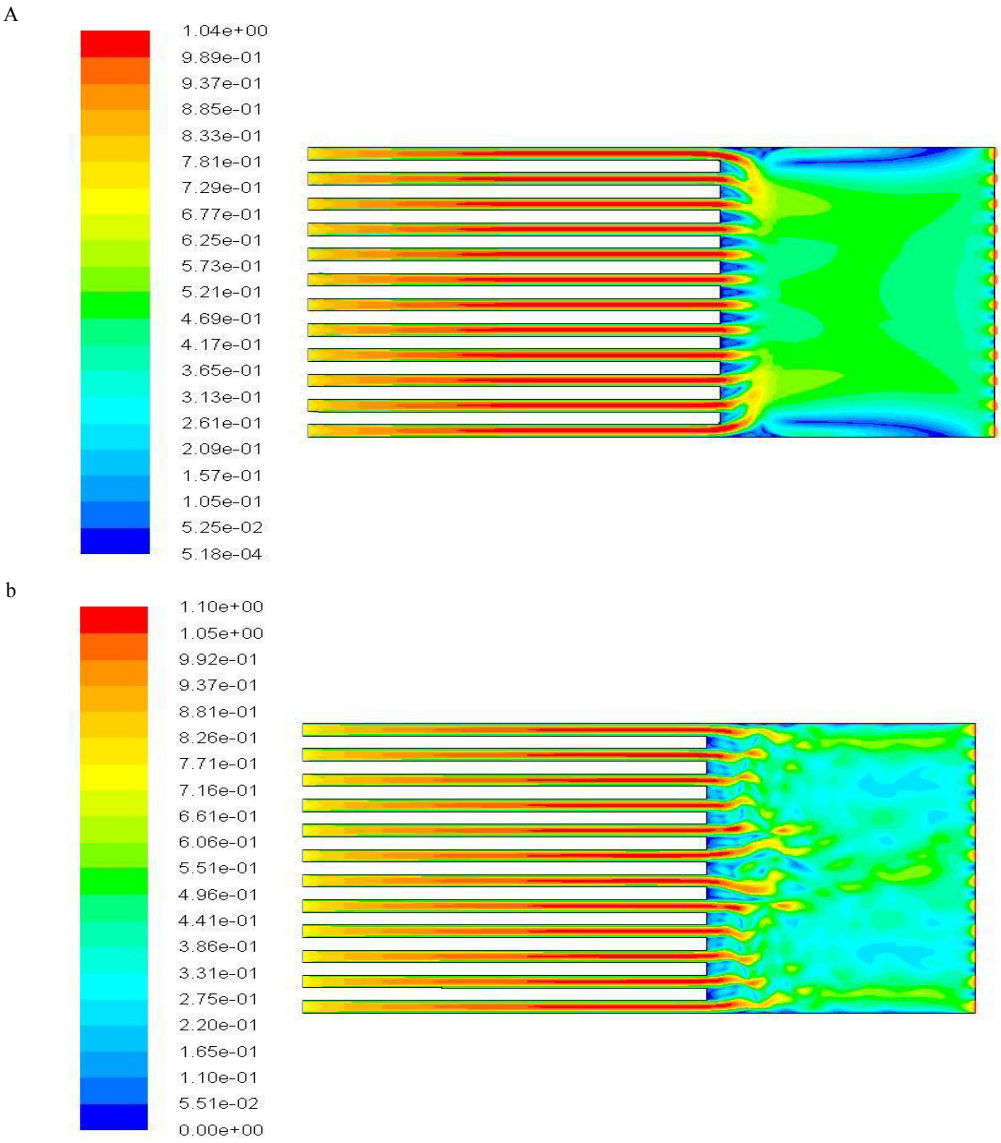


Fig. 8. Velocity contours of micro-channel and profile region in (a) transition and (b) laminar flow conditions.

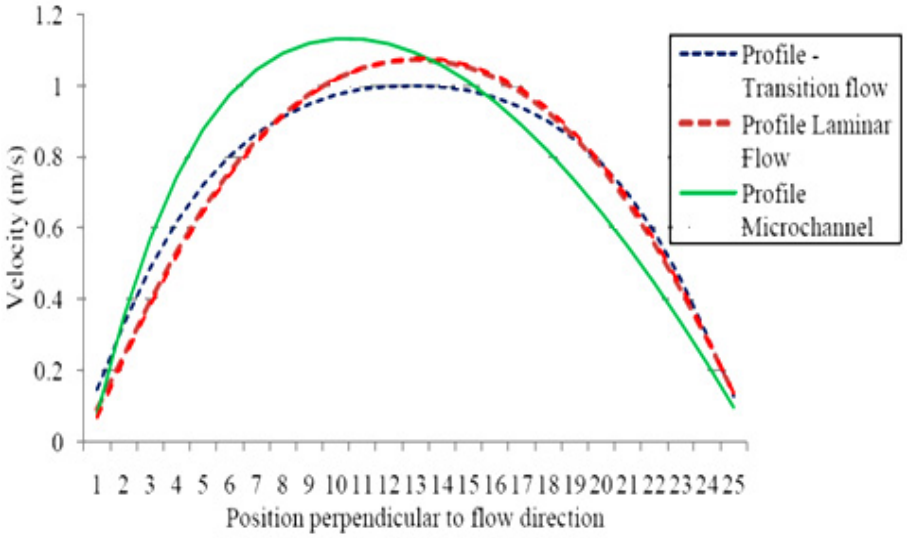


Fig. 9.Velocity profile at micro channel outlets for different flow conditions.

### *2.6. Configuration of cooling module design*

In order to improve the temperature uniformity, the flow pattern in the module should ideally in the form of a spiral. Now based on the micro-channel performance data we have, it is assumed that average rise in temperature of bottom plate over a micro-channel array is around 2°C. The module consists of 36 such micro-channel arrays. The inlet water temp is 40°C and $T_{min}$ of module = 45°C.From table 5.1 we can say that either 3 or 6 inlets is the preferred choice for module flow arrangement in order to generate maximum electricity. The flow arrangement possible with 3 and 6 inlets are shown below in Fig. 10 (a-c). With 3 inlets fluid has to make 6 turns and 6 inlets no turns are required. Having turns leads to higher pressure drop across the channel and might also result in turbulence. Hence for final design a no turn design (6 inlets) with all inlets on one edge is selected. The other design with alternate inlet and outlet will result in better heat uniformity overall but manufacturing alternating inlet outlet ports for the overall module will complicate the design for the flow distribution mechanism and hence is not selected.

a

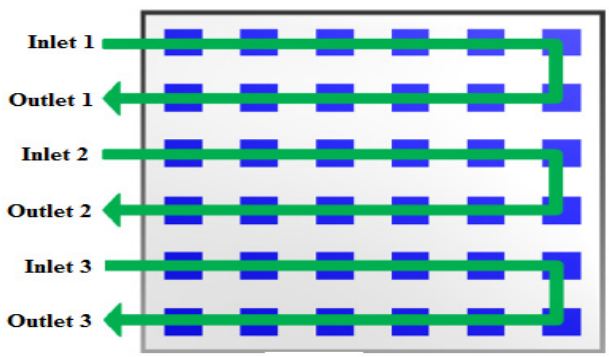

b

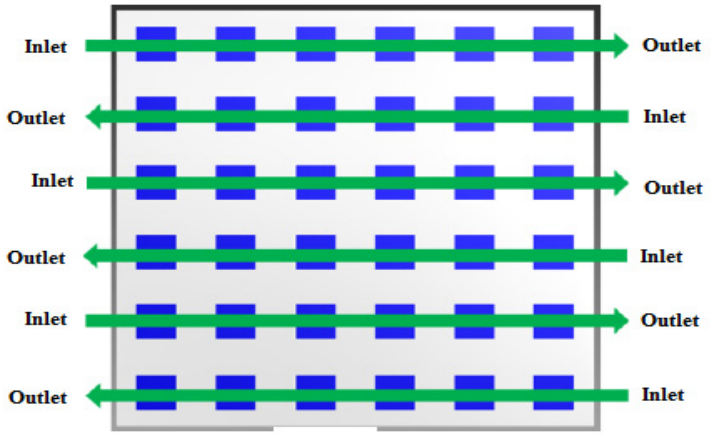


c

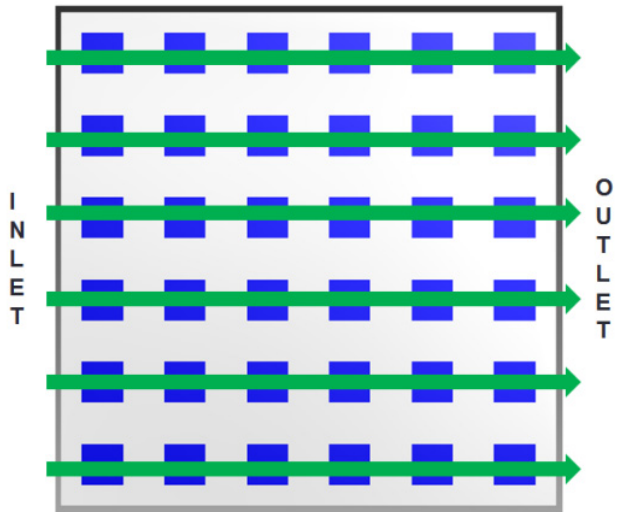


Fig.10. Flow arrangements patterns (a) 3-inlets U flow (b) 6-inlets with alternate flow direction (cross flow) (c) 6-inlets with same flow direction

### *2.7. Description of cooling module design*

A single cooling module consists of heat sink surface on its back side and multi junction cells mounted on its front side. The whole heat sink surface is a combination of four individual square modules of size 120mm x 120mm as shown in Fig. 11. Hence the overall size of the cooling module is 240mm x 240mm. Each module can be viewed as a combination of 6 symmetric parallel flow channels more clearly visible in Fig. 12. Each channel can be viewed as a combination of 13 regions (6 micro channels, 5 profile regions, 1-inlet and 1-outlet profile).

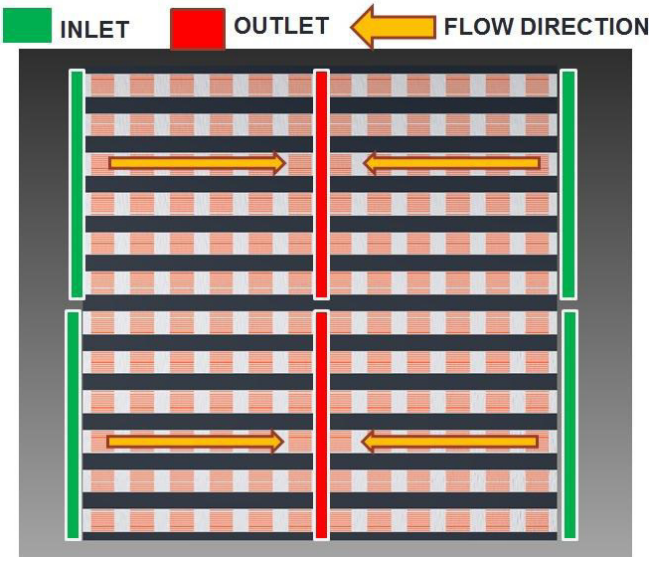


Fig.11. Flow arrangements for complete module

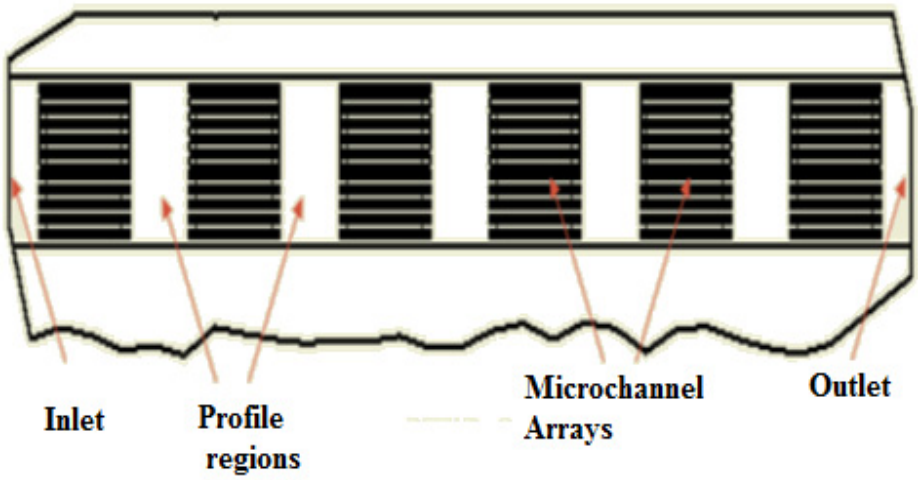


Fig. 12. Single symmetric parallel channel.

*2.8. Temperature and Pressure distributions in micro-channel*

Due to symmetry one parallel channel geometry was modeled, meshed and analyzed to predict the temperature distribution over one module, which in turn would be sufficient for predicting temperature distribution over the entire heat sink. Numerical simulations were conducted for13 different regions namely 6 micro-channels arrays, 5 profile regions of 8 mm and 4 mm length with inlet and outlet.

For Volume flow rate of 0.0176 litter/s, the overall temperature difference of bottom surface ($\Delta T$) is 9.09 K ($T_{max}$ = 322.09, $T_{min}$ = 313 K) and the water temperature difference is 5.53 K ($T_{max}$ = 317.53, $T_{min}$ = 313 K) with a pressure drop of 8.680 k Pa overall across channel, resulting in the pumping requirement of 4 Watts for the full module. The

corresponding average temperature difference for micro channel array is 1.67 K with Temperature uniformity index ($U_T$) over micro channel array of 0.48 K.

The cumulative pressure drop of coolant along the flow is shown in Fig. 13. (a). The pressure profile along the flow direction is mostly linear in nature. The fluid velocity along the flow direction is shown in Fig. 13. (b). As represented by flat lines the average flow velocity remains constant inside the micro-channel, the flow accelerates in the profile region then slows down and at the end the again accelerates because it moves from an area of 1mm width to 0.5 mm width. The effect of the pressure drop with in profile region is shown in Fig. 14. Both the pressure drop and flow velocity in micro channel array is increasing linearly with micro-channel number. Due to flow constriction at micro channel inlet in the profile region, the flow velocity increases at micro channel entry resulting in increased pressure drop in micro channel array.

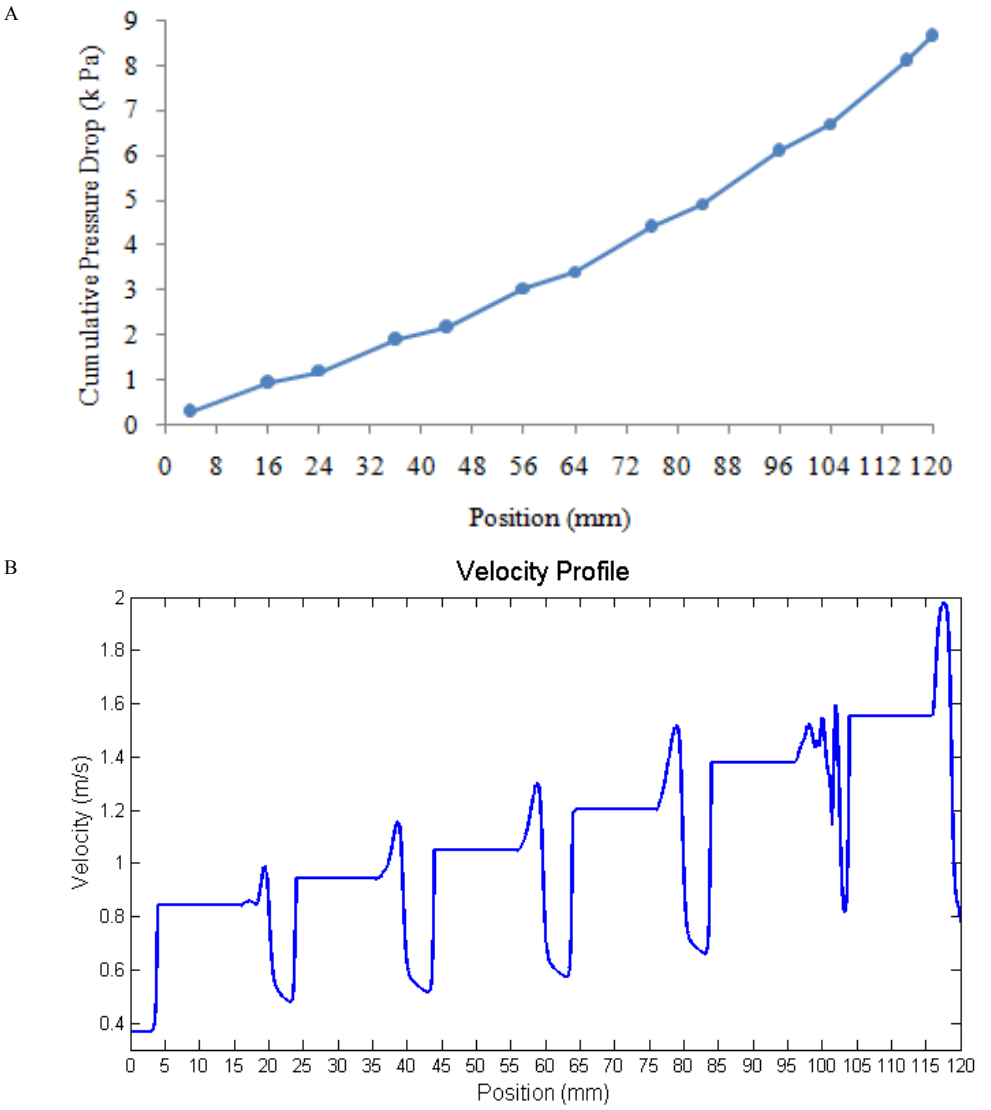


Fig. 13. Variation of (a) pressure and (b) velocity of coolant flow in micro channel

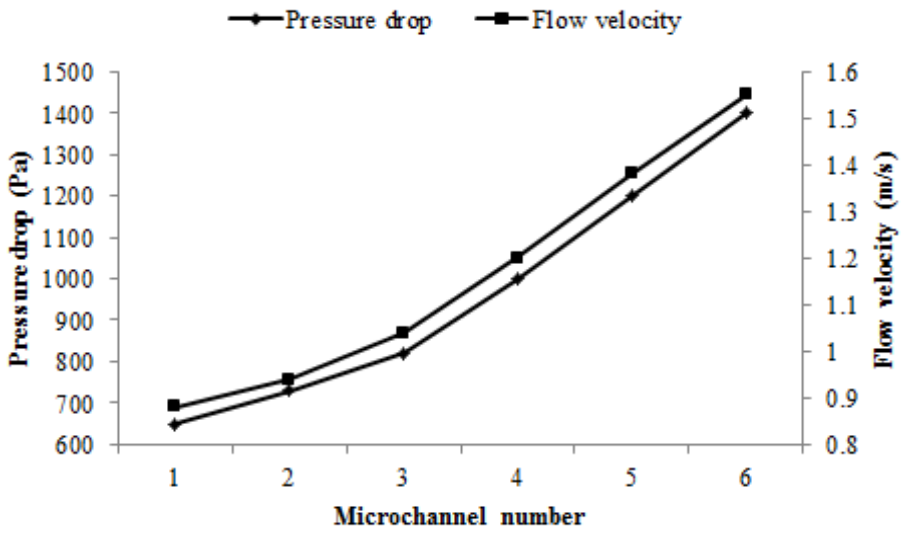


Fig. 14. Flow velocity and pressure drop for different profile regions

The spatial temperature variation on the bottom surface of heat sink along the flow direction is shown in Fig. 15. (a).The reason for sudden dip in temperature profile and contour is due to the fact that separate simulations are done for micro-channel and profile region. The profile region does not have any heat generation and hence at steady state the bottom temperature of the profile region is equal to the average temperature of water, which in turn is less than the exit bottom surface temperature of the micro channel. The variation of water temperature with the fin height along the flow direction is shown in Fig. 15. (b). The temperature of bottom, middle and top surface are in descending order with most of the heat being taken away by the bottom surface.

A

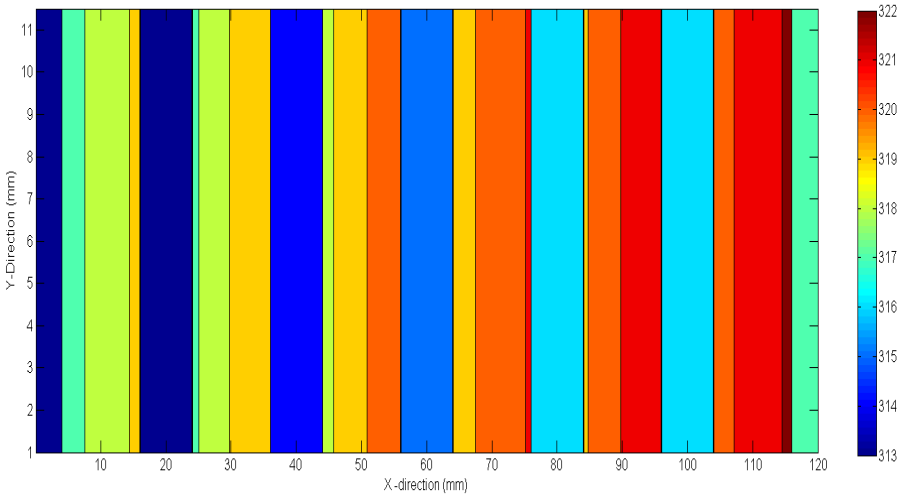

B

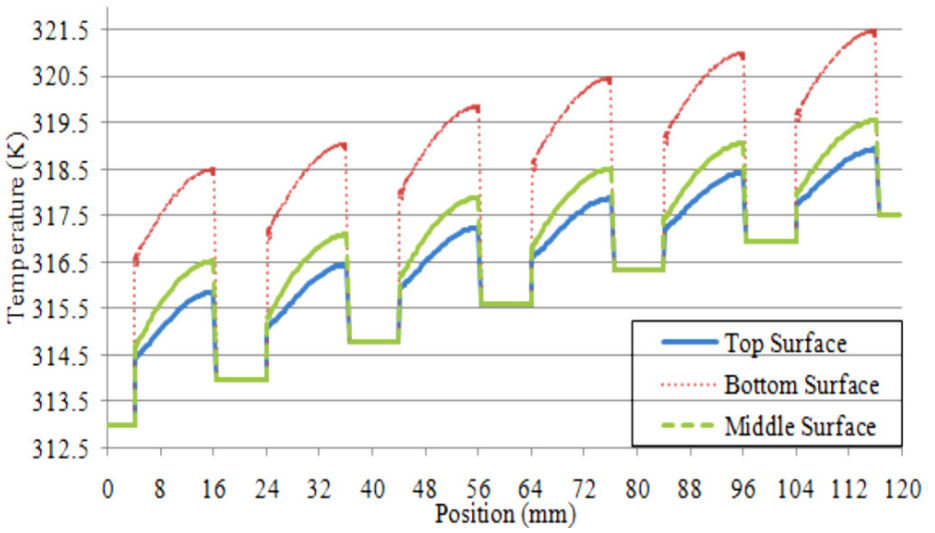


Fig. 15. (a) Temperature variation and contour of bottom face of heat sink; (b) Temperature profile of surface of water along fin height with the flow direction.

## 3. Conclusions

Investigation of channel cooling technologies employing different flow arrangement, for CPV cooling has been carried out. The micro channels were found to better at cooling the module and pressure drop was found to be low in straight flow channels, both these facts were combined to develop a combinatory model with micro channel array removing heat and straight flow channels providing the flow direction. It was found that micro channels with higher aspect ratios, lower widths and higher Re result in a low temperature rise of bottom surface and high temperature uniformity index. As flow progresses in the straight channel containing micro channels its velocity increases which in turn result in better heat transfer in later micro channels with similar amount of temperature rise and temperature uniformity even with higher inlet temperature. The optimized geometry of micro channel for the CPV receiver was found to be W=0.5 mm, Length = 12mm and Pitch = 0.5mm. The final results predicts over less than 10 K rise in temperature of CPV module of dimensions 240 x 240 $mm^2$, with a pressure drop of 8.8 kPa along a single channel with six such channels in each modules at a flow rate of 0.105 lit/s. The overall load was calculated to be 4 W which is approximately 0.2% of the power produced by the CPV module.

## References

[1] Leonardo Micheli, Nabin Sarmah, Xichun Luo, K.S. Reddy, Tapas K Mallick, Opportunities and challenges in micro-and nano-technologies for concentrating photovoltaic cooling: A review, Renewable and Sustainable Energy Reviews, 2013; 20: pp. 595–610.
[2] Royne, C.J. Dey and D.R. Mills, Cooling of photovoltaic cells under concentrated illumination: a critical review. Solar Energy Materials and Solar Cells, 2005; 86(4): pp. 451-483.
[3] Verlinden, P.,Sinton, R.A., Swanson, R.M., Crane, R.A., Single-wafer integrated 140 W silicon concentrator module, Photovoltaic Specialists Conference, 1991., Conference Record of the Twenty Second IEEE 1991; vol. 1;739 - 743.
[4] Lasich, J.B., Cooling circuit for receiver of solar radiation. Patent no. WO02080286; 2002.
[5] Vincenzi, D., Bizzi, F., Stefancich, M., Malagu, C., Morini, G.L., Antonini, A. and Martinelli, G., Micro-machined silicon heat exchanger for water cooling of concentrator solar cells. PV in Europe Conference and Exhibition - From PV technology to Energy Solutions, Rome 2002.
[6] Min, J.Y., Jang, S.P. and Kim, S.J., Effect of tip clearance on the cooling performance of a micro-channel heat sink. International Journal of Heat and Mass Transfer 47 (5), 2004; 1099-1103.
[7] Lee, D.-Y. and Vafai, K., Comparative analysis of jet impingement and micro-channel cooling for high heat flux applications. International Journal of Heat and Mass Transfer 42 (9), 1999; 1555-1568.
[8] Ryu, J.H., Choi, D.H. and Kim, S.J., Three-dimensional numerical optimization of a manifold micro-channel heat sink. International Journal of Heat and Mass Transfer 46 (9), 2003; 1553-1562.
[9] Bejan, A., Heat Transfer, John Wiley & sons, Inc., Singapore; 1993.